STEM CELLS TRANSLATIONAL MEDICINE®

PROTOCOLS AND MANUFACTURING FOR CELL-BASED THERAPIES

Rapid and Efficient Directed Differentiation of Human Pluripotent Stem Cells Into Retinal Pigmented Epithelium

DAVID E. BUCHHOLZ,[a,b,c] BRITNEY O. PENNINGTON,[a,b,c] ROXANNE H. CROZE,[a,b,c] CASSIDY R. HINMAN,[a,b] PETER J. COFFEY,[a,b,d] DENNIS O. CLEGG[a,b,c,d]

Key Words. Cellular therapy • Differentiation • Embryonic stem cells • Pluripotent stem cells • Induced pluripotent stem cells • Retinal pigmented epithelium

[a]Center for Stem Cell Biology and Engineering, [b]Neuroscience Research Institute, [c]Department of Molecular, Cellular and Developmental Biology, and [d]Center for the Study of Macular Degeneration, University of California, Santa Barbara, California, USA

Correspondence: Dennis O. Clegg, Ph.D., Neuroscience Research Institute, University of California, Santa Barbara, California 93106, USA. Telephone: 805-893-8490; Fax: 805-893-2005; E-Mail: clegg@lifesci.ucsb.edu; or Peter J. Coffey, D.Phil., Neuroscience Research Institute, University of California, Santa Barbara, California 93106, USA. Telephone: 805-893-4621; Fax: 805-893-2005; E-Mail: peter.coffey@lifesci.ucsb.edu

Received November 28, 2012; accepted for publication February 12, 2013; first published online in SCTM *EXPRESS* April 18, 2013.

1066-5099/2013/$20.00/0

http://dx.doi.org/10.5966/sctm.2012-0163

ABSTRACT

Controlling the differentiation of human pluripotent stem cells is the goal of many laboratories, both to study normal human development and to generate cells for transplantation. One important cell type under investigation is the retinal pigmented epithelium (RPE). Age-related macular degeneration (AMD), the leading cause of blindness in the Western world, is caused by dysfunction and death of the RPE. Currently, RPE derived from human embryonic stem cells are in clinical trials for the treatment of AMD. Although protocols to generate RPE from human pluripotent stem cells have become more efficient since the first report in 2004, they are still time-consuming and relatively inefficient. We have found that the addition of defined factors at specific times leads to conversion of approximately 80% of the cells to an RPE phenotype in only 14 days. This protocol should be useful for rapidly generating RPE for transplantation as well as for studying RPE development in vitro. STEM CELLS TRANSLATIONAL MEDICINE *2013;2:000–000*

INTRODUCTION

Age-related macular degeneration (AMD) is the leading cause of blindness in the aging population of the Western world [1]. AMD presents in two forms, wet and dry, caused by dysfunction and death of the retinal pigmented epithelium (RPE) through mechanisms still being resolved [2]. The wet form, characterized by neovascularization, can be effectively treated with monthly injections of antiangiogenic drugs such as Lucentis (Genentech, South San Francisco, CA, http://www.gene.com). Although effective, there is substantial cost and inconvenience associated with monthly injections into the back of the eye [3]. The dry form of AMD is characterized by drusenoid aggregates under the basal side of the RPE at early stages, which progresses to geographic atrophy with marked loss of RPE and photoreceptors. Currently there is no effective treatment for the dry form of AMD, which accounts for 80%–90% of AMD cases.

Because the etiology of AMD is still under investigation, one focus of therapy has been on replacing diseased RPE through transplantation [4]. The feasibility of this approach has been demonstrated by autologous replacement of RPE in the macula, the central portion of the retina responsible for high acuity vision, via macular translocation or relocation of peripheral RPE to the macula [5–7]. Although somewhat effective, these surgeries are long and complicated. The derivation of RPE from pluripotent cells and their efficacy in preclinical models of retinal degeneration have led to the design of simpler transplantation strategies that are much faster and cost-effective. Two methods of transplantation predominate: a subretinal bolus injection of single cells and subretinal insertion of a patch of RPE grown in its native monolayer form [8, 9]. Currently, clinical trials are under way using RPE derived from human embryonic stem cells (hESCs) using the bolus injection approach, with clinical trials using the patch soon to follow.

The translation of pluripotent stem cell-derived RPE has moved rapidly toward the clinic, and researchers in the lab have also been working to increase both the speed and efficiency of RPE derivation. Initial work on human pluripotent stem cell RPE began when it was observed that hESCs allowed to "spontaneously" differentiate would give rise to a low percentage of RPE, easily identifiable by pigmentation; this work was later recapitulated with induced pluripotent stem cells [10–12]. This is the paradigm currently being used to generate RPE for the clinic. Although reliable, it is extremely inefficient and time-consuming, with an efficiency of ~1% after 1–2 months in culture (although this varies between lines). RPE are typically not harvested until

after 2–3 months in culture, to give pigmented foci time to expand. A major breakthrough in the directed differentiation of pluripotent stem cells to RPE came in 2010 when the addition of nicotinamide and Activin A was shown to increase the efficiency of RPE generation to 33% after 6 weeks as determined by the number of pigmented cells [13]. The highest reported efficiency of RPE generation was obtained by exposing pluripotent cells to basic fibroblast growth factor (bFGF), Noggin, retinoic acid, and Shh. An efficiency of ~60% $Mitf^{+}$ cells after 60 days of differentiation was reported [14].

Interestingly, a report in 2006 showed that neural retinal progenitors could be generated with ~80% efficiency after 21 days of differentiation through the application of a handful of factors (insulin-like growth factor 1 [IGF1], Noggin, Dkk1, and bFGF) [15]. Because RPE and the neural retina arise from a common progenitor pool [16], we sought to determine whether this protocol could be altered to direct pluripotent stem cells to RPE with a similar efficiency. Through the combined use of the retinal inducing factors (IGF1, Noggin, Dkk1, and bFGF) and other factors (nicotinamide, Activin A, SU5402, and vasoactive intestinal peptide [VIP]) added at appropriate times, we have found that pluripotent stem cells could be directed to RPE with an efficiency of ~80% based on Pmel17 expression. Importantly, these cells could be isolated as early as 14 days following the onset of differentiation. This protocol should be useful for quickly generating quantities of RPE for transplantation as well as for the study of RPE development.

Materials and Methods

Pluripotent Stem Cell Culture

The human embryonic stem cell line H9 (WiCell Research Institute, Madison, WI, http://www.wicell.org) was maintained in Dulbecco's Modified Eagle's Medium: Nutrient Mixture F-12 (DMEM/F12) containing 2 mM GlutaMAX-I, 20% knockout serum replacement, 0.1 mM Modified Eagle's Medium Non-Essential Amino Acids (MEM NEAA), 0.1 mM β-mercaptoethanol (Invitrogen, Carlsbad, CA, http://www.invitrogen.com) and 4 ng/ml bFGF (Peprotech, Rocky Hill, NJ, http://www.peprotech.com) on a mitomycin C (Sigma-Aldrich, St. Louis, MO, http://www.sigmaaldrich.com)-treated mouse embryonic fibroblast feeder layer. H9s for flow cytometry were grown on growth factor-reduced Matrigel (BD Biosciences, San Diego, CA, http://www.bdbiosciences.com) in mTESR1 (StemCell Technologies, Vancouver, BC, Canada, http://www.stemcell.com) medium. The human embryonic stem cell line UCSF4 (NIH registry no. 0044, University of California, San Francisco) was maintained on growth factor-reduced Matrigel (BD Biosciences) in mTESR1 medium (StemCell Technologies). The induced pluripotent stem cell line iPS(IMR90)-4 (IMR904) (kind gift of J. Thomson, University of Wisconsin and University of California, Santa Barbara) was maintained in DMEM/F12 containing 2 mM GlutaMAX-I, 20% knockout serum replacement, 0.1 mM MEM NEAA, 0.1 mM β-mercaptoethanol (Invitrogen) and 100 ng/ml recombinant zebrafish bFGF (gift of J. Thomson) on a mitomycin C (Sigma-Aldrich)-treated mouse embryonic fibroblast feeder layer.

Differentiation Into Retinal Pigmented Epithelium

Pluripotent stem cells were passaged directly onto Matrigel (BD Biosciences) in DMEM/F12 with 1× B27, 1× N2, and 1× NEAA (Invitrogen). From days 0 to 2, 50 ng/ml Noggin, 10 ng/ml Dkk1, and 10 ng/ml IGF1 (R&D Systems Inc., Minneapolis, MN, http://www.rndsystems.com) and in some experiments 10 mM nicotinamide or 5 mM 3-aminobenzamide (Sigma-Aldrich) were added to the base medium. From days 2 to 4, 10 ng/ml Noggin, 10 ng/ml Dkk1, 10 ng/ml IGF1, and 5 ng/ml bFGF and in some experiments 10 mM nicotinamide or 5 mM 3-aminobenzamide were added to the base medium. From days 4 to 6, 10 ng/ml Dkk1 and 10 ng/ml IGF1 and in some experiments 100 ng/ml Activin A (R&D Systems) were added to the base medium. From days 6 to 14, 100 ng/ml Activin A, 10 μM SU5402 (EMD Millipore, Darmstadt, Germany, http://www.emdmillipore.com), and 1 mM VIP (Sigma-Aldrich) were added to the base medium. Control experiments were also performed in base media alone (DMEM/F12, B27, N2, and NEAA).

The cells were mechanically enriched by scraping away cells with non-RPE morphology. Subsequently, the remaining RPE were digested using TrypLE Express (Invitrogen) for ~5 minutes at 37°C. The cells were passed through a 30-μm single-cell strainer and seeded onto Matrigel-coated tissue culture plastic, Transwell membranes (Corning Enterprises, Corning, NY, http://www.corning.com), or CC2-treated chambered slides. Enriched cells were cultured in DMEM-high glucose with 1% fetal bovine serum (FBS), GlutaMAX, and sodium pyruvate (Invitrogen) for 30 days [17].

Hs27 and cultured fetal human RPE (kind gift of D. Bok) were cultured on Matrigel-coated Transwell membranes in DMEM-high glucose with 1% FBS, GlutaMAX, and sodium pyruvate (Invitrogen). MeWo cells were cultured in DMEM/F12 GlutaMAX1 (Invitrogen) with 10% fetal bovine serum (HyClone, Logan, UT, http://www.hyclone.com).

Quantitative Real-Time Polymerase Chain Reaction

Total RNA was isolated using the RNeasy Plus Mini Kit (Qiagen, Hilden, Germany, http://www.qiagen.com). cDNA was synthesized from 1 μg of RNA using the iScript cDNA Synthesis Kit (Bio-Rad, Hercules, CA, http://www.bio-rad.com). Primer pairs were designed to create a 75–200-base pair product (Beacon Design 4.0; Premier Biosoft International, Palo Alto, CA, http://www.premierbiosoft.com). Quantitative real-time polymerase chain reaction (PCR) was carried out on a Bio-Rad MyIQ Single Color Real-Time PCR Detection System using the SYBR Green method [18]. Triplicate 20-μl reactions were run in a 96-well plate with half of the cDNA synthesis reaction used per plate. Primer specificity was confirmed by melting temperature analysis, gel electrophoresis, and direct sequencing (Iowa State DNA Facility, Ames, IA). The data were normalized to the geometric mean of the "housekeeping" genes: glyceraldehyde phosphate dehydrogenase (*GAPDH*), hydroxymethylbilane synthase (*HMBS*), and glucose phosphate isomerase (*GPI*) [19]. The primer sequences are listed in supplemental online Table 1.

Immunocytochemistry

The cells were grown on Matrigel-coated 12-well tissue culture plates (days 0–14) or enriched onto Matrigel-coated chambered slides and cultured for 1 month. For fixation, the plates and slides were washed with phosphate-buffered saline (PBS), fixed with 4% paraformaldehyde in 0.1 M sodium cacodylate buffer, pH 7.4, for 15 minutes at 4°C, and stored in PBS at 4°C until labeling. The slides were washed with PBS, blocked with PBS containing 5% BSA and 0.1% NP40 in PBS for 1 hour at 4°C, treated with ice-cold

90% methanol for 5 minutes, and incubated with primary antibodies (listed in supplemental online Table 1) overnight at 4°C. The slides were incubated with an appropriate Alexa Fluor (Invitrogen)-conjugated secondary antibody (1:300) for 30 minutes at 4°C, stained with Hoechst (2 μg/ml) (Invitrogen) for 5 minutes at room temperature, washed with PBS, and then imaged at room temperature using an Olympus IX71 fluorescence microscope or an Olympus Fluoview FV10i confocal microscope (Olympus, Center Valley, PA, http://www.olympusamerica.com). The antibodies used are listed in supplemental online Table 2.

Flow Cytometry

The samples were fixed in 4% paraformaldehyde in PBS (Electron Microscopy Sciences, Hatfield, PA, http://www.emsdiasum.com/microscopy) and permeabilized with 0.2% Triton X-100 (Roche, Indianapolis, IN, http://www.roche.com). The samples were labeled with primary or isotype control antibodies for 30 minutes at 4°C. Primary and isotype control antibodies that were not conjugated to fluorophores were labeled with fluorophore-conjugated secondary antibodies for 30 minutes at 4°C. The labeled samples were run on an Accuri C6 flow cytometer with CFlow collection software (BD Biosciences). Data analysis was performed on FCS Express 4 Flow Research Edition (De Novo Software, Thornhill, ON, Canada, http://www.denovosoftware.com). The positive percentage was based on a background level set at 1% positive expression in samples labeled with isotype control antibodies.

Rod Outer Segment Phagocytosis

Rod outer segment (ROS) phagocytosis assays were performed as previously described [20]. Bovine eyes were obtained fresh from Sierra Medical Inc. (Whittier, CA, http://www.sierra-medical.com); ROSs were purified from retinal extracts and fluorescently labeled using the FluoReporter FITC Protein Labeling Kit (Invitrogen). The cells were seeded in quadruplicate on gelatin-coated wells in a 96-well plate at a concentration of 25,000–50,000 cells per well and allowed to grow to confluence for 4 weeks. The cells were then challenged with 1×10^6 fluorescein isothiocyanate-labeled ROSs per well with or without 50 μg/ml anti-$\alpha v\beta 5$ (ab24694; Abcam, Cambridge, U.K., http://www.abcam.com) or 50 μg/ml IgG1 control (ab9404; Abcam) for 5 hours at 37°C in 5% CO_2. The wells were then vigorously washed five times with warm PBS to remove unbound ROSs. To determine the level of ROS internalization, an equal volume of 0.4% trypan blue was added to the PBS for 10 minutes to quench extracellular fluorescence. Trypan blue was aspirated, and 40 μl of PBS was added to the well to prevent the cells from drying out. The internalized ROSs were then documented in fluorescence photomicrographs. Fluorescence intensity was quantified by pixel densitometry using ImageJ software (National Institutes of Health, Bethesda, MD) for photomicrograph analysis. Photomicrographs from three wells for each condition were averaged within each assay. Separate experiments were normalized to the positive control ARPE-19 cell line, which was assayed in each experiment.

Results

Nicotinamide Speeds Up Early Eye Field Differentiation

Because nicotinamide had previously been shown to increase differentiation of RPE from pluripotent stem cells [13], we tested whether nicotinamide would influence differentiation at early stages of eye field development. In this first segment of differentiation, cell clumps are mechanically dissected from pluripotent stem cell colonies and seeded on Matrigel in the presence of IGF1, Noggin, and DKK1. On day 2, bFGF is added. The addition of nicotinamide to IGF1, Noggin, Dkk1, and bFGF significantly decreased expression of the pluripotency genes Oct4 and Nanog on day 4 compared with controls (Fig. 1A, 1B). Expression of early neural/early eye field markers Lhx2 and Rax increased in the presence of nicotinamide on day 4 compared with controls; however, the increase in Rax was not significant (Fig. 1B). Interestingly, Pax6(−5a) expression was similar between nicotinamide and control conditions (Fig. 1B). Cells in the presence of nicotinamide rapidly adopted a radial/rosette morphology compared with control cells, which still contained a large percentage of cells with undifferentiated morphology (Fig. 1C). Control cells expanded more rapidly than cells in nicotinamide.

Nicotinamide can have many effects on cultured cells, including inhibition of poly(ADP-ribose) polymerase (PARP), which can protect cells from oxidative stress [13, 21]. To examine the mechanism of nicotinamide induced differentiation, we tested the ability of 3-aminobenzamide, an inhibitor of PARP, to recapitulate the effects of nicotinamide. 3-Aminobenzamide reduced levels of Oct4 and Nanog compared with controls on day 4, but not as much as nicotinamide (Fig. 1B). Similarly, 3-aminobenzamide significantly increased levels of Lhx2 and Rax compared with controls on day 4, but not as much as nicotinamide (Fig. 1B). Overall, 3-aminobenzamide was able to partially recapitulate the effects of nicotinamide.

Activin A, SU5402, and VIP Direct Early Eye Field Cells to an RPE Fate

Following the acquisition of early eye field markers by day 4 (Fig. 1B), we sought to direct the cell to RPE instead of neural retina. With this in mind, we phased out the addition of nicotinamide (added days 0–4), Noggin (added days 0–4), bFGF (added days 2–4), IGF1 (added days 0–6), and Dkk1 (added days 0–6) and tested the effect of Activin A, SU5402, and VIP on RPE specification.

The addition of Activin A on days 4–10 had little effect on gene expression of Mitf, a marker of the optic vesicle and of RPE. Expression of Rax, a marker of the early eye field and neural retina, was significantly decreased (Fig. 1D). Addition of SU5402 on days 6–10 had little effect on expression of either Mitf or Rax; however, in combination with Activin A, expression of Rax was further decreased (Fig. 1D). VIP has been previously shown to speed up maturation of cultured primary RPE by increasing intracellular cAMP and activating pp60(c-src) [22]. Addition of VIP on days 6–10 significantly increased expression of RPE marker genes Mitf, tyrosinase, and PEDF (Fig. 1E). Consistent with the roles of Mitf and tyrosinase in pigment synthesis, pigmentation was increased in cultures containing VIP between days 10 and 14 (data not shown). By day 10, sheets of cells with cobblestone morphology and distinct borders were visible (Fig. 1F; supplemental online Fig. 2A, 2B).

Differentiation to RPE Is Highly Efficient

Following 4 more days in culture with Activin A, SU5402, and VIP, the borders of cobblestone sheets became more defined, and some cells began to pigment (Fig. 2A; supplemental online Fig. 2A, 2B). Immunocytochemistry for the melanosomal protein

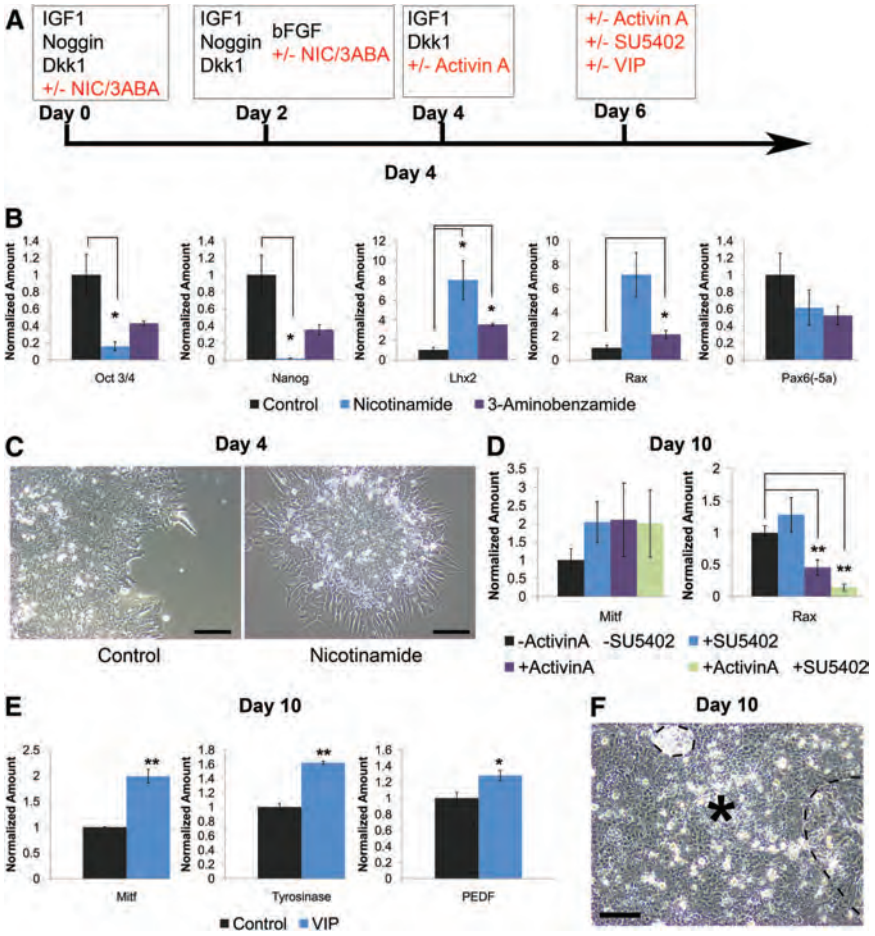

Figure 1. Defined factors rapidly direct pluripotent cells toward an early eye field and retinal pigmented epithelium fate. **(A):** Timing of factor addition. The factors in red were under investigation. **(B):** The effect of nicotinamide and 3-aminobenzamide on pluripotency and early eye field gene expression. mRNA levels were quantified by polymerase chain reaction (qPCR) and normalized to the control condition (IGF1, Noggin, DKK1, and bFGF at the times shown in **[A]**). The error bars represent the standard error of the mean. *, $p \leq .1$. **(C):** The effect of nicotinamide on cell morphology. Phase contrast images are shown. Scale bars = 200 μm. **(D):** The effect of Activin A and SU5402 alone and in combination on Mitf and Rax gene expression. mRNA levels were quantified by qPCR and normalized to the control condition (IGF1, Noggin, DKK1, bFGF, and nicotinamide at the times shown in **[A]**). The error bars represent the standard error of the mean. **(E):** The effect of VIP on retinal pigmented epithelium gene expression. mRNA levels were quantified by qPCR and normalized to the control condition (IGF1, Noggin, DKK1, bFGF, nicotinamide, Activin A, and SU5402 at the times shown in **[A]**). The error bars represent the standard error of the mean. **, $p \leq$ .05. **(F):** Morphology at day 10 following the addition of IGF1, Noggin, DKK1, bFGF, nicotinamide, Activin A, SU5402, and VIP at the times shown in **(A)**. The asterisk marks an area with cobblestone morphology. Scale bar = 200 μm. Abbreviations: bFGF, basic fibroblast growth factor; IGF, insulin-like growth factor; VIP, vasoactive intestinal peptide.

Pmel17 (upon which melanin pigment is deposited) exclusively labeled these pigmenting sheets of cells (Fig. 2A). Quantitative polymerase chain reaction (qPCR) analysis showed that compared with cells differentiated in B27/N2 containing basal medium only (no factor differentiation), cells that had been exposed to RPE differentiation factors (nicotinamide, IGF1, DKK1, Noggin, bFGF, Activin A, SU5402, and VIP) had significantly increased levels of the RPE marker genes Mitf, Tyrosinase, Tyrp2, PEDF, BEST1, and Pmel17 (Fig. 2B). Additional immunocytochemistry revealed Mitf expression exclusively in pigmenting sheets of cells, whereas Lhx2 and ZO1 could be found in both pigmenting sheets and non-RPE cells (Fig. 2C). Interestingly, in addition to Lhx2, some non-RPE cells expressed Oct4 (supplemental online Fig. 1B). When isolated and replated in pluripotent stem cell conditions, these cells did not form colonies with typical undifferentiated stem cell morphology, and many appeared to differentiate into neurons (supplemental online Fig. 2C).

To determine the efficiency of differentiation, we performed flow cytometry using the Pmel17 antibody, which is highly sensitive and which labels only pigmenting sheets of cells by immunocytochemistry. We also examined the loss of the pluripotency marker Oct4 by flow cytometry. We found that H9 cells could be differentiated into Pmel17$^+$ cells by day 14 with an average efficiency of 78.5% ($\pm$1.2%, n = 6, H9-RPE) (Fig. 2D). This was highly significant when compared with either undifferentiated H9 cells (12.8% $\pm$ 2.4%, n = 3, H9) or cells differentiated in basal medium alone (25.2% $\pm$ 1.6%, n = 3, no factor differentiation) (Fig. 2D). We tested the differentiation protocol on two additional pluripotent stem cell lines: the embryonic stem cell line UCSF4 and the induced pluripotent stem cell line IMR904. The UCSF4 line yielded Pmel17$^+$ cells with an efficiency similar to H9 cells (79.8% $\pm$ 0.88%, n = 3, UCSF4-RPE), whereas the IMR904 line was slightly less efficient (63% $\pm$ 0.88%, n = 3, IMR904-RPE) (Fig. 2D). The percentage of Oct4$^+$ cells was less than 5% in all

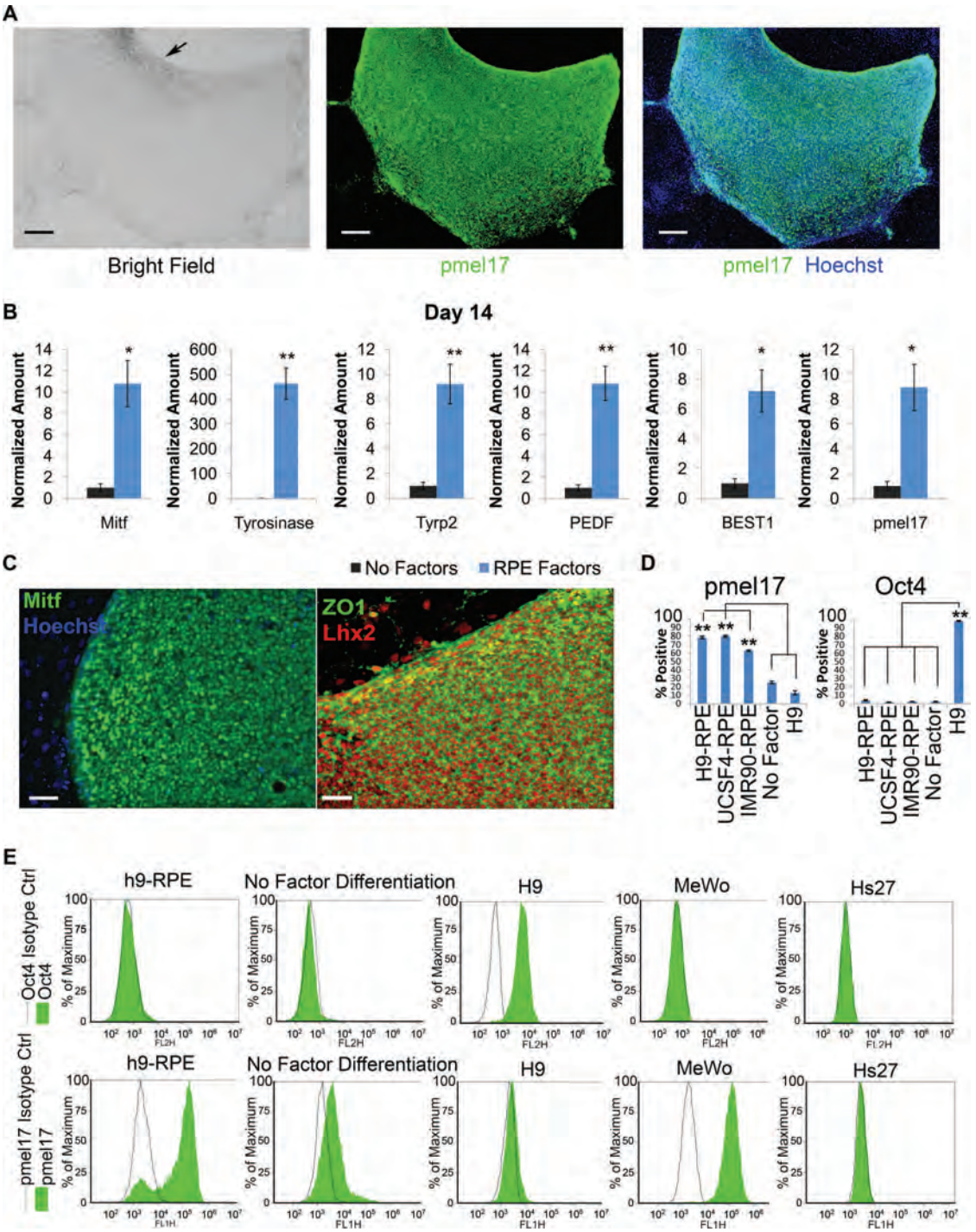

Figure 2. Sheets of RPE progenitors are efficiently generated and begin to pigment by day 14 of differentiation. **(A):** Bright field and immunofluorescence images of a sheet of RPE at day 14. The arrow points to pigmented cells. Scale bars = 500 μm. **(B):** RPE gene expression following differentiation in insulin-like growth factor 1, Noggin, DKK1, basic fibroblast growth factor, nicotinamide, Activin A, SU5402, and vasoactive intestinal peptide compared with differentiation in basal medium alone. mRNA levels were quantified by quantitative polymerase chain reaction and normalized to the no factor condition (differentiated in B27/N2 DMEM/F12 medium). The error bars represent the standard error of the mean. *, $p \leq .1$; **, $p \leq .05$. **(C):** Immunofluorescence images of RPE sheets at day 14. Scale bar = 100 μm. **(D):** Quantification of Pmel17 and Oct4 immunoreactivity by flow cytometry after 14 days differentiation of H9, UCSF4, and IMR90, compared with undifferentiated H9. The error bars represent the standard error of the mean. **, $p \leq .05$. **(E):** Representative flow cytometry histograms for Pmel17 and Oct4 at day 14 (H9-RPE, H9 no factor differentiation), undifferentiated H9 cells, MeWo cells (positive control for Pmel17), and Hs27 cells (negative control for both Pmel17 and Oct4). Abbreviations: Ctrl, control; RPE, retinal pigmented epithelium.

conditions except undifferentiated H9 cells (98.1% ± 0.6%, n = 3, H9) (Fig. 2D).

Examination of representative flow cytometry histograms reveals population expression levels of Pmel17 and Oct4 protein on day 14. We compared H9-RPE cells differentiated in basal media (no factor differentiation), undifferentiated H9 cells, the melanocyte cell line MeWo (a positive control for Pmel17), and the fibroblast line Hs27 (a negative control for both Oct4 and Pmel17). Interestingly, undifferentiated H9 cells appeared to express low levels of Pmel17 (Fig. 2E). This is consistent with findings in our own lab and others that undifferentiated stem cells express low levels of this transcript [11, 23]. A high level of Pmel17 protein expression was only seen in H9-RPE cells and the positive control MeWo cells (melanocytes) (Fig. 2E).

Interestingly, cells left in culture past day 14 with Activin A, SU5402, and VIP led to death of non-RPE cells (supplemental online Fig. 2A, 2B). This suggests that the culture conditions are both directive and selective for RPE. Because one of our goals was to determine the earliest time we could generate homogenous cultures of RPE, we focused on day 14 as the end point of directed differentiation.

Protein and mRNA Time Courses Reveal Stages of RPE Development

To better understand the nature of our differentiation protocol, we analyzed both protein and mRNA expression of a panel of genes over 14 days of differentiation. As expected, pluripotency gene and protein expression (Oct4 and Nanog) decreased rapidly over the first 4 days (Fig. 3A, 3B). Interestingly, Oct4 and Nanog expression increased slightly between days 4 and 6, during which time Activin A was added to the protocol (Fig. 3B). Early neural and eye field markers (Lhx2, Pax6(−5a), Pax6(+5a), and Rax) were expressed as early as day 2, with expression increasing throughout the 14-day time period with the exception of Rax (Fig. 3A, 3B). Rax expression was transient, increasing from days 2–6 and then rapidly decreasing between days 6 and 8 (Fig. 3B). At day 6, IGF1 and DKK1 were removed from the protocol, whereas SU5402 and VIP were added, which could account for the decrease in Rax expression. RPE marker genes were expressed slightly later in two phases, between days 4 and 6 (Mitf, PEDF, and BEST1) and between days 6 and 8 (Pmel17, Tyrosinase, and Tyrp2) (Fig. 3A, 3B). Interestingly, Otx2 mRNA and protein were expressed at relatively consistent levels throughout differentiation.

Differentiated Cells Can Be Enriched on Day 14 to Homogenous Cultures of Functional RPE

To generate more homogenous populations of RPE, readily visible sheets on day 14 were mechanically isolated, dissociated into single cells, and replated in an RPE medium [17] on Matrigel-coated tissue culture plastic, chambered slides, or Transwell inserts. Surprisingly, RPE enriched on day 14 were sensitive to singe-cell dissociation in the media tested, leading to cell death or senescence (supplemental online Fig. 2D). Because the Rho-associated protein kinase (ROCK) inhibitor Y27632 has been previously shown to support single-cell dissociation of epithelial cells [24–26], including pluripotent stem cells [27], we tested the ability of this small molecule to rescue dissociated RPE. The addition of Y27632 at 10 μM for the first 3 days after passage facilitated RPE survival and maturation (Fig. 4; supplemental online Fig. 2D).

After enriching RPE at day 14, we allowed the cells to redifferentiate for 30 days and then analyzed gene and protein expression and phagocytosis of rod outer segments. To analyze gene expression, hESC-RPE, cultured fetal human RPE (fRPE), and Hs27 fibroblasts were cultured on Transwell inserts for 30 days. qPCR analysis showed similar levels of expression of all RPE marker genes between hESC-RPE and fRPE (Fig. 4A). We used Hs27 cells as a negative control for RPE-specific genes; however, we detected some Mitf, PEDF, and BEST1 expression in Hs27. Compared with undifferentiated H9 cells, expression of Oct4 was ~1,000-fold lower in all other cell lines (Fig. 4A).

Immunocytochemistry of cells enriched at day 14 and grown on chambered slides for 30 days showed homogenous populations of RPE based on Mitf, Otx2, Lhx2, ZO1, and Pmel17 expression (Fig. 4B). Expression of BEST1 and RPE65, markers of more mature RPE, was heterogeneous, indicating varying levels of maturity in these cultures (Fig. 4B). Integrin αv was localized apically compared with Otx2 nuclear expression, showing proper polarized protein trafficking in these cells (Fig. 4B, inset in Integrin αv/Otx2 panel). Although some Oct4$^+$ cells were present at day 14 of initial differentiation, no Oct4$^+$ cells were observed following enrichment and 30 days of culture (Fig. 4B).

To determine whether our hESC-RPE were functional, we tested their ability to carry out phagocytosis of fluorescently labeled ROSs. Compared with the negative control Hs27 cells, hESC-RPE internalized significantly more ROSs (Fig. 4C). This internalization was blocked by an antibody against integrin αvβ5, showing that both hESC-RPE and fRPE use the same receptor for ROS phagocytosis. hESC-RPE ROS phagocytosis was even greater than that of fRPE, although both RPE lines internalized significantly more ROSs than Hs27 cells.

Discussion

The challenge of efficiently directing pluripotent stem cells into a specific lineage has progressed rapidly since the derivation of human embryonic stem cells 15 years ago [28, 29]. Development of efficient protocols to generate RPE, which are the second hESC derivative used in clinical trials, has been progressing since initial reports of spontaneous differentiation 8 years ago [10, 13, 14, 30]. Here we report a protocol that is both fast and efficient. By drawing upon knowledge from developmental biology and other stem cell studies, we have optimized timing of factor addition to generate RPE within 14 days.

Nicotinamide has previously been used to differentiate pluripotent stem cells into RPE [13]. It was shown that nicotinamide had an antiapoptotic effect following 2 weeks of differentiation, in line with other studies showing neural protection by nicotinamide. Based on previous research, it was suggested that this action could be through inhibition of poly(ADP-ribose) polymerase-1 (PARP1), which was found to regulate cell death upon hESC neural induction [21]. In our experiments, the addition of nicotinamide to retinal inducing factors IGF1, DKK1, Noggin, and bFGF [15] decreased expression of pluripotency genes while concomitantly increasing neural/early eye field genes by day 4. Because it is known that the IGF1, DKK1, Noggin, and bFGF protocol induces expression of Lhx2, Rax, and Pax6 [15], these gene expression changes suggest that the addition of nicotinamide speeds up differentiation. Interestingly, not all neural/early eye field genes were affected by nicotinamide. Although Lhx2 and Rax expression increased with nicotinamide addition on day 4,

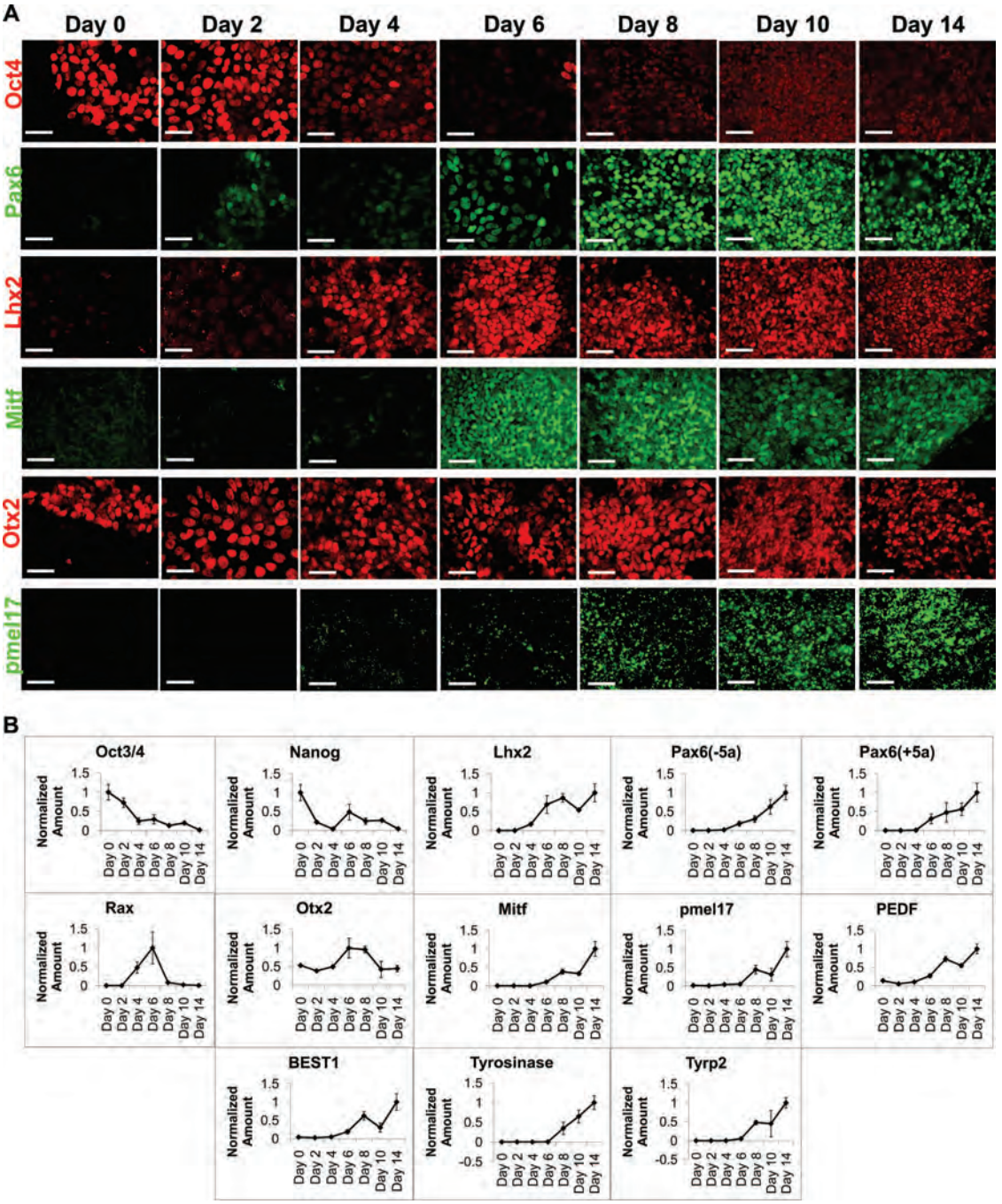

Figure 3. Differentiating cells rapidly acquire early eye field and retinal pigmented epithelium (RPE) marker expression. **(A):** Immunofluorescence images of pluripotency (Oct4), early eye field (Pax6, Lhx2, and Otx2), and RPE (Pax6, Lhx2, Mitf, Otx2, and Pmel17) proteins during days 0–14 of differentiation. Scale bars = 100 μm. **(B):** Quantitative polymerase chain reaction analysis of pluripotency (Oct4 and Nanog), early eye field (Lhx2, Pax6(−5a), Pax6(+5a), Rax, and Otx2), and RPE (Lhx2, Pax6(−5a), Pax6(+5a), Otx2, Mitf, Pmel17, PEDF, BEST1, Tyrosinase, and Tyrp2) gene expression. Expression is normalized to the maximum level of expression over the time period. The error bars represent the standard error of the mean.

Pax6 expression was slightly lower, although this change was not significant. This suggests that nicotinamide may not have an effect on Pax6 and may act on a factor downstream. Further studies are needed to elucidate the effect of nicotinamide-expedited differentiation on the entire early eye field transcription factor network (Pax6, Lhx2, Rax, Six3, Six6, and Tll [31]). We also saw fewer cells in nicotinamide conditions, which could result from either cell death or a decrease in proliferation. A decrease in proliferation has previously been reported upon exposure of hESCs to nicotinamide [32]. Although these results suggest a role for nicotinamide outside of cell survival, we wondered whether PARP1 inhibition was still involved. To test the role of PARP1 inhibition in our nicotinamide induced differentiation, we tested the ability of another PARP1 inhibitor, 3-aminobenzamide, to induce differentiation. We found that 3-aminobenzamide could partially recapitulate the effects seen with nicotinamide.

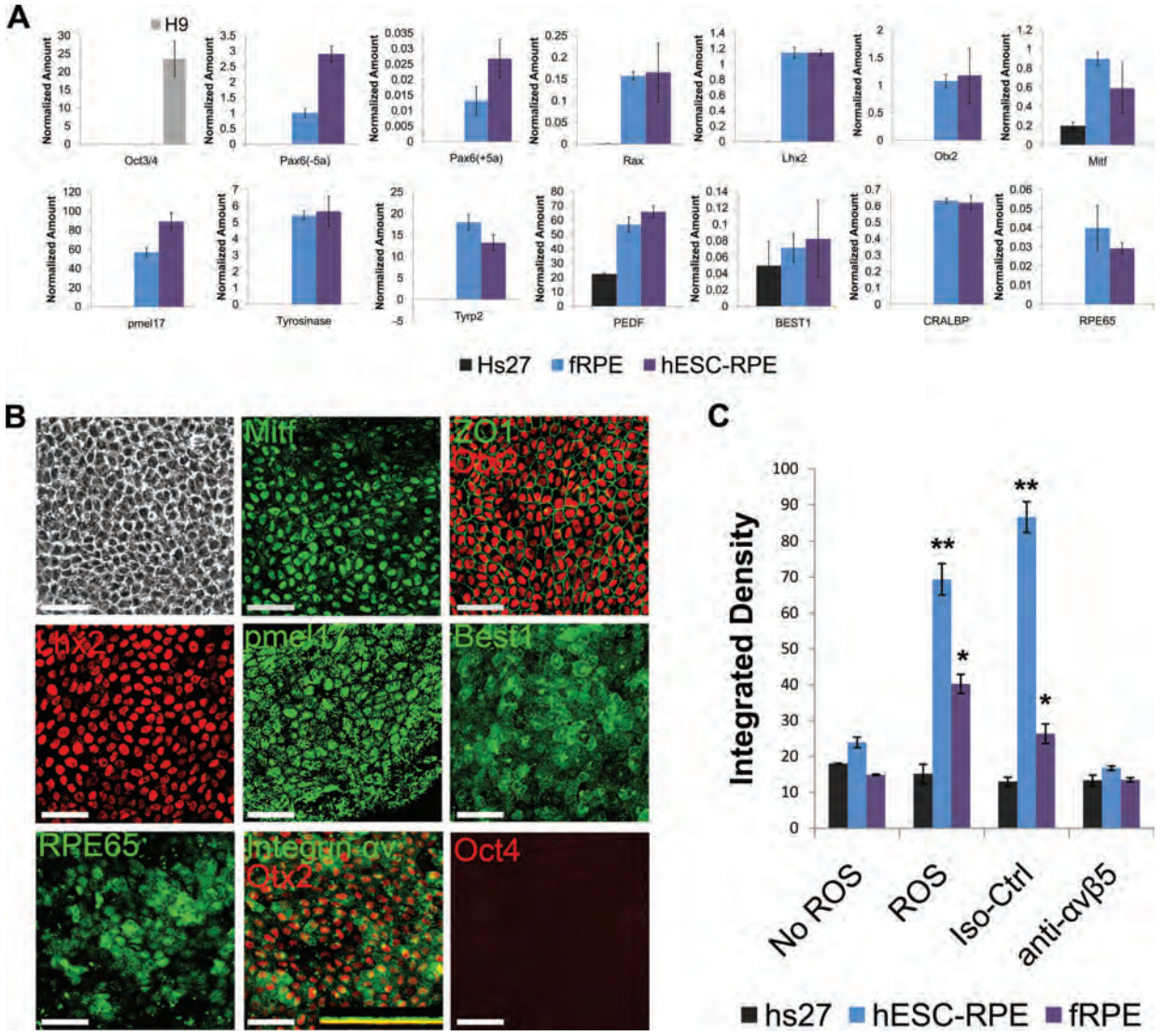

Figure 4. Analysis of RPE enriched on day 14 and grown for 30 days in culture. **(A):** Quantitative polymerase chain reaction analysis comparing gene expression levels in hESC-RPE to cultured fetal human RPE as a positive control and Hs27 cells as a negative control. Undifferentiated H9 cells are included as a positive control for Oct4 expression in the first panel. Expression is normalized to a panel of housekeeping genes. The error bars represent the standard error of the mean. **(B):** Bright field and immunofluorescent labeling of RPE and pluripotency markers. The inset in the Integrin av/Otx2 panel shows the confocal *z*-stack cross-section. Scale bars = 50 μm. **(C):** Internalization of fluorescently labeled ROSs quantified by integrated pixel density analysis of fluorescent images. The error bars represent the standard error of the mean. *, $p \leq .05$; **, $p \leq .01$ versus respective Hs27 control and corresponding anti-$\alpha v\beta 5$ condition. Abbreviations: anti-$\alpha v\beta 5$, function blocking integrin $\alpha v\beta 5$ antibody; fRPE, fetal human retinal pigmented epithelium; hESC, human embryonic stem cell; Iso-Ctrl, isotype control antibody; RPE, retinal pigmented epithelium; ROS, rod outer segment.

Although the exact mechanism of nicotinamide-induced neuronal differentiation remains to be elucidated, it is clear that nicotinamide can potentiate differentiation, and this potentiation appears to act at least partially through PARP inhibition. Neuroprotective/antiapoptotic effects of PARP inhibition may also play a role. We find that nicotinamide is a useful tool to speed up initial neural differentiation and could potentially be applied to other neural differentiation protocols.

The addition of Activin A and the FGFR1 inhibitor SU5402 led to only slight increases in RPE genes, whereas the early eye field/neural retina marker Rax was significantly downregulated by day 10. We attribute the former to the potent retinal inducing properties of IGF1 [15, 33], whereas the latter confirms the roles of Activin A and FGF signaling in the optic vesicle to optic cup stages of eye development. This is seen in both animal and hESC models where Activin signaling and FGF inhibition direct the progenitor cells toward RPE (Rax^{-}) instead of neural retina (Rax^{+}) [13, 16, 30]. The addition of VIP significantly increases expression of Mitf, Tyrosinase, and PEDF, in agreement with results found in primary cultures of RPE [22]. Although we continued to use VIP for these experiments and indeed saw an increase in pigmentation at earlier time points, the use of VIP at 1 mM can be quite expensive. For practical purposes, VIP can be left out of the protocol.

By day 14 of differentiation, sheets of RPE can clearly be seen with defined borders that express several RPE marker genes and proteins. By this time cells have begun to pigment. Interestingly, the speed of pigmentation appears to be inversely correlated

with the efficiency of RPE differentiation or size of the RPE sheet (data not shown). Small sheets ($<$500 μm) tended to pigment faster than large sheets ($>$5 mm). This suggests that signals coming from non-RPE cells may have a positive effect on pigmentation. Future studies will be necessary to determine what those signals may be.

Generation of RPE from both H9 and UCSF4 embryonic stem cell lines was highly efficient, averaging close to 80% based on Pmel17 immunoreactivity. This method induced efficient differentiation of RPE in the UCSF4 cell line, which is resistant to RPE differentiation using the spontaneous method (data not shown). The efficiency of RPE generation from IMR904 induced pluripotent stem (iPS) cells was somewhat less efficient at 60%. The cause of this difference in efficiency is unclear, although it could be due to incomplete silencing of the reprogramming transgenes. It will be interesting to see whether the efficiency is consistently lower in iPS cells compared with embryonic stem cells, although we do not suspect this to be the case.

Cells that did not express Pmel17 on day 14 of differentiation expressed Oct4 and Lhx2. When isolated on day 14 and placed back in embryonic stem cell conditions, these cells did not form colonies that resembled embryonic stem cell morphology, and many appeared to differentiate into neurons. We suspect that these cells may be stuck in a partially differentiated state. If differentiating cultures were kept longer than 14 days, these non-RPE cells began to die. We therefore consider the Activin A-, SU5402-, and VIP-supplemented medium to both direct differentiation and select for RPE over non-RPE cells, leading to virtually homogenous populations of RPE after 3 weeks.

Analysis of gene and protein expression throughout the 14-day differentiation period revealed several interesting trends. First, as expected, early neural and eye field genes were expressed first, followed by later markers of the optic vesicle and RPE [16]. Interestingly, although gene expression followed the known developmental sequence, transition from early eye field to optic vesicle and RPE was quite rapid. This suggests that during normal development, the ability of a cell to respond to developmental cues can precede those signals by a significant amount of time, perhaps to allow time for tissue growth. Between days 4 and 6, a slight increase in Oct4 and Nanog gene expression was observed. We believe this is likely because of the addition of Activin A on day 4 because Activin A signaling has been shown to maintain pluripotency [34–36]. Consistent with recent observations in Rax-GFP pluripotent stem cells undergoing ocular morphogenesis [37, 38], we saw transient expression of Rax between days 2 and 8. This would appear to correspond with expression in the early eye field followed by downregulation in the RPE. Interestingly, Otx2, which has been shown to be repressed by Rax specifically in the early eye field of *Xenopus* [31], maintained a fairly consistent level of both mRNA and protein expression over the 14-day time course. In fact, Otx2 mRNA expression increased when Rax mRNA expression was at its highest. These observations, along with results from other hESC retinal differentiation protocols [30], suggest that Otx2 is expressed in the early eye field of humans. Alternatively, there are two known protein isoforms of Otx2 in humans and several different transcripts, which may be alternatively regulated. Our experiments do not differentiate between these isoforms. There is also the possibility that maintained Otx2 expression throughout ocular differentiation may be an artifact of cell culture and may not be found in vivo.

Because morphologically distinct sheets of RPE became visible between days 10 and 14, we tried to isolate cells at these early time points. Initial attempts were unsuccessful; however, with the addition of the ROCK inhibitor Y27632 over the first few days of culture, RPE could be enriched at both of these time points and would mature into functional RPE when replated. The borders of RPE sheets at day 10 were harder to distinguish, which made enrichment to homogenous populations difficult; therefore we focused on enrichment at day 14. Tight junctions among non-RPE cells made them easy to remove as sheets by dragging a pipette tip along borders with RPE.

ROCK inhibition has been used successfully to maintain survival of hESCs dissociated into single cells as well as to enhance proliferation of certain epithelial cell types [24–27]. The mechanism of ROCK inhibition has been worked out in hESCs, where ROCK mediates E-cadherin cell adhesion sensing [39]. The mechanism of ROCK inhibition in proliferation of other epithelial cell types, including in our own system, remains to be elucidated. Primary RPE cultures, when dissociated into single cells over several passages, lose their ability to redifferentiate into mature RPE and become fibroblastic in morphology. This may be a wound response for an epithelium that does not normally exist as single cells and may be similar to the effect we see following single-cell dissociation on day 14 of differentiation. Additionally, our selection of basal medium may not be optimal for proliferating cultures of RPE enriched at day 14. We are currently testing novel medium compositions, some of which support single-cell growth even in the absence of ROCK inhibitor. Although the mechanism is not known, enrichment of RPE cells on day 14 in the presence of ROCK inhibitor can generate homogenous populations that express RPE marker genes at similar levels to cultured fetal human RPE, express proper RPE proteins, are polarized, and display integrin $\alpha v\beta 5$-dependent phagocytosis of rod outer segments.

Conclusion

This protocol should be useful for studying human ocular differentiation within a shorter time period than in vivo development. Signals that specify melanogenesis in RPE are still under investigation. Our observation that cultures with more non-RPE cells led to faster RPE pigmentation suggests that these cells may secrete factors that activate melanogenesis. Analysis of the proteome of these non-RPE cells may lead to identification of melanogenic factors. This protocol will also be useful for rapidly generating banks of RPE for the treatment of age-related macular degeneration and other disorders of the RPE.

Acknowledgments

We thank Sherry Hikita and Monte Radeke for their guidance and the University of California, Santa Barbara, Center for Stem Cell Biology and Engineering staff for support. This work was supported by Grants CL1-00521, DR1-01444, FA1-006161, and TG2-01151 from the California Institute for Regenerative Medicine (CIRM). B.O.P. was supported by a CIRM scholarship, and P.J.C. was supported by a CIRM Leadership Award. Further support was provided by the Institute for Collaborative Biotechnologies through Grant W911NF-09-0001 from the U.S. Army Research Office. The content of the information does not necessarily reflect the position or the policy of the government, and no official endorsement should be inferred.

Author Contributions

D.E.B.: conception and design, collection and/or assembly of data, data analysis and interpretation, manuscript writing, final approval of manuscript; B.O.P., R.H.C., and C.R.H.: conception and design, collection and/or assembly of data, data analysis and interpretation, final approval of manuscript; P.J.C. and D.O.C.: conception and design, financial support, final approval of manuscript.

Disclosure of Potential Conflicts of Interest

A U.S. patent application has been filed for the protocol reported herein. D.O.C. has compensated honoraria and uncompensated research funding from Allergan. D.O.C. is a cofounder of Regenerative Patch Technologies (uncompensated employment and uncompensated ownership interest) and also has uncompensated intellectual property rights and is an uncompensated consultant for Regenerative Patch Technologies.

References

1 Khandhadia S, Cherry J, Lotery AJ. Age-related macular degeneration. Adv Exp Med Biol 2012;724:15–36.

2 Anderson DH, Radeke MJ, Gallo NB et al. The pivotal role of the complement system in aging and age-related macular degeneration: Hypothesis re-visited. Prog Retin Eye Res 2010;29:95–112.

3 Cruess AF, Berger A, Colleaux K et al. Canadian expert consensus: Optimal treatment of neovascular age-related macular degeneration. Can J Ophthalmol 2012;47:227–235.

4 Rowland TJ, Buchholz DE, Clegg DO. Pluripotent human stem cells for the treatment of retinal disease. J Cell Physiol 2012;227:457–466.

5 Chen FK, Uppal GS, MacLaren RE et al. Long-term visual and microperimetry outcomes following autologous retinal pigment epithelium choroid graft for neovascular age-related macular degeneration. Clin Experiment Ophthalmol 2009;37:275–285.

6 Chen FK, Patel PJ, Uppal GS et al. A comparison of macular translocation with patch graft in neovascular age-related macular degeneration. Invest Ophthalmol Vis Sci 2009;50:1848–1855.

7 Chen FK, Patel PJ, Uppal GS et al. Long-term outcomes following full macular translocation surgery in neovascular age-related macular degeneration. Br J Ophthalmol 2010;94:1337–1343.

8 Schwartz SD, Hubschman JP, Heilwell G et al. Embryonic stem cell trials for macular degeneration: A preliminary report. Lancet 2012; 379:713–720.

9 Hu Y, Liu L, Lu B et al. A novel approach for subretinal implantation of ultrathin substrates containing stem cell-derived retinal pigment epithelium monolayer. Ophthalmic Res 2012; 48:186–191.

10 Klimanskaya I, Hipp J, Rezai KA et al. Derivation and comparative assessment of retinal pigment epithelium from human embryonic stem cells using transcriptomics. Cloning Stem Cells 2004;6:217–245.

11 Buchholz DE, Hikita ST, Rowland TJ et al. Derivation of functional retinal pigmented epithelium from induced pluripotent stem cells. Stem Cells 2009;27:2427–2434.

12 Carr AJ, Vugler AA, Hikita ST et al. Protective effects of human iPS-derived retinal pigment epithelium cell transplantation in the retinal dystrophic rat. PLoS One 2009;4:e8152.

13 Idelson M, Alper R, Obolensky A et al. Directed differentiation of human embryonic stem cells into functional retinal pigment epithelium cells. Cell Stem Cell 2009;5:396–408.

14 Zahabi A, Shahbazi E, Ahmadieh H et al. A new efficient protocol for directed differentiation of retinal pigmented epithelial cells from normal and retinal disease induced pluripotent stem cells. Stem Cells Dev 2012;21:2262–2272.

15 Lamba DA, Karl MO, Ware CB et al. Efficient generation of retinal progenitor cells from human embryonic stem cells. Proc Natl Acad Sci USA 2006;103:12769–12774.

16 Martínez-Morales JR, Rodrigo I, Bovolenta P. Eye development: A view from the retina pigmented epithelium. Bioessays 2004;26:766–777.

17 Ahmado A, Carr AJ, Vugler AA et al. Induction of differentiation by pyruvate and DMEM in the human retinal pigment epithelium cell line ARPE-19. Invest Ophthalmol Vis Sci 2011;52:7148–7159.

18 Woo TH, Patel BK, Cinco M et al. Identification of *Leptospira biflexa* by real-time homogeneous detection of rapid cycle PCR product. J Microbiol Methods 1999;35:23–30.

19 Radeke MJ, Peterson KE, Johnson LV et al. Disease susceptibility of the human macula: Differential gene transcription in the retinal pigmented epithelium/choroid. Exp Eye Res 2007;85:366–380.

20 Lin H, Clegg DO. Integrin alphavbeta5 participates in the binding of photoreceptor rod outer segments during phagocytosis by cultured human retinal pigment epithelium. Invest Ophthalmol Vis Sci 1998;39:1703–1712.

21 Cimadamore F, Curchoe CL, Alderson N et al. Nicotinamide rescues human embryonic stem cell-derived neuroectoderm from parthanatic cell death. Stem Cells 2009;27:1772–1781.

22 Koh SM. VIP enhances the differentiation of retinal pigment epithelium in culture: From cAMP and pp60(c-src) to melanogenesis and development of fluid transport capacity. Prog Retin Eye Res 2000;19:669–688.

23 Sperger JM, Chen X, Draper JS et al. Gene expression patterns in human embryonic stem cells and human pluripotent germ cell tumors. Proc Natl Acad Sci USA 2003;100:13350–13355.

24 Chapman S, Liu X, Meyers C et al. Human keratinocytes are efficiently immortalized by a Rho kinase inhibitor. J Clin Invest 2010;120: 2619–2626.

25 Liu X, Ory V, Chapman S et al. ROCK inhibitor and feeder cells induce the conditional reprogramming of epithelial cells. Am J Pathol 2012;180:599–607.

26 Okumura N, Koizumi N, Ueno M et al. ROCK inhibitor converts corneal endothelial cells into a phenotype capable of regenerating in vivo endothelial tissue. Am J Pathol 2012; 181:268–277.

27 Watanabe K, Ueno M, Kamiya D et al. A ROCK inhibitor permits survival of dissociated human embryonic stem cells. Nat Biotechnol 2007;25:681–686.

28 Ben-David U, Kopper O, Benvenisty N. Expanding the boundaries of embryonic stem cells. Cell Stem Cell 2012;10:666–677.

29 Thomson JA, Itskovitz-Eldor J, Shapiro SS et al. Embryonic stem cell lines derived from human blastocysts. Science 1998;282:1145–1147.

30 Meyer JS, Shearer RL, Capowski EE et al. Modeling early retinal development with human embryonic and induced pluripotent stem cells. Proc Natl Acad Sci USA 2009;106:16698–16703.

31 Zuber ME, Gestri G, Viczian AS et al. Specification of the vertebrate eye by a network of eye field transcription factors. Development 2003;130:5155–5167.

32 Vaca P, Berna G, Araujo R et al. Nicotinamide induces differentiation of embryonic stem cells into insulin-secreting cells. Exp Cell Res 2008;314:969–974.

33 Pera EM, Wessely O, Li SY et al. Neural and head induction by insulin-like growth factor signals. Dev Cell 2001;1:655–665.

34 Beattie GM, Lopez AD, Bucay N et al. Activin A maintains pluripotency of human embryonic stem cells in the absence of feeder layers. Stem Cells 2005;23:489–495.

35 Xiao L, Yuan X, Sharkis SJ. Activin A maintains self-renewal and regulates fibroblast growth factor, Wnt, and bone morphogenic protein pathways in human embryonic stem cells. Stem Cells 2006;24:1476–1486.

36 Vallier L, Alexander M, Pedersen RA. Activin/nodal and FGF pathways cooperate to maintain pluripotency of human embryonic stem cells. J Cell Sci 2005;118:4495–4509.

37 Eiraku M, Takata N, Ishibashi H et al. Self-organizing optic-cup morphogenesis in three-dimensional culture. Nature 2011;472:51–56.

38 Nakano T, Ando S, Takata N et al. Self-formation of optic cups and storable stratified neural retina from human ESCs. Cell Stem Cell 2012;10:771–785.

39 Ohgushi M, Sasai Y. Lonely death dance of human pluripotent stem cells: ROCKing between metastable cell states. Trends Cell Biol 2011;21:274–282.

See www.StemCellsTM.com for supporting information available online.